Fault Self-Organization as Optimal Random Paths Selected by Critical Spatiotemporal Dynamics of Earthquakes

Philippe Miltenberger, Didier Sornette, and Christian Vanneste
Laboratoire de Physique de la Matière Condensée, Université de Nice-Sophia Antipolis, Parc Valrose, 06108 Nice Cedex 2, France
(Received 27 April 1993)

We study a simple 2D dynamical model of a tectonic plate with long-range elastic forces and quenched disorder. The interplay between long-range elasticity, threshold dynamics, and the quenched featureless small-scale heterogeneity allows us to capture both the spontaneous formation of fractal fault structures by repeated earthquakes and a short-time spatiotemporal chaotic dynamics of earthquakes, well described by a Gutenberg-Richter power law. Faults are mapped onto a minimal interface problem, which in 2D corresponds to the random directed polymer problem and are thus self-affine with a roughness exponent $\frac{2}{3}$.

PACS numbers: 91.30.Dk, 05.40.+j, 64.60.Ht, 91.45.−c

Geological deformation and faulting are the long-term cumulative traces of short-term processes such as earthquakes [1–4]. Earthquakes occur on faulted zones which are in turn progressively organized by the accumulation of rupture events. The mechanism behind this self-organization and the precise relationship between these largely different time scales are still lacking (see, however, [5]). An understanding of this problem is essential both for a better characterization of geological structures and for earthquake prediction purposes. An important open question is whether the spatial and temporal complexity of earthquakes and fault structures emerge from geometrical and material built-in heterogeneities [6] or from the chaotic behavior [7,8] inherent to the nonlinear equations governing the dynamics of these phenomena.

Here, we address this question through a detailed analysis of a simple 2D dynamical model of a tectonic plate with long-range elastic forces. Except for the crucial introduction of quenched disorder, our model is similar to that of Ref. [9] and is a direct extension of Ref. [10] obtained by introducing "healing" after each rupture or slip event. In the present version [11], it simulates antiplane scalar shear deformation along the axis $0z$ of a thin tectonic plate placed in the x-y plane. The plate is discretized in a network of L by L elements or plaquettes oriented at 45° with respect to the edges. The 2D lattice represents a thin 2D tectonic plate at scales larger than its thickness. A constant slow antiplane velocity along $0z$ is applied at the boundaries to simulate the effect of neighboring plates. Periodic boundary conditions are applied along the two edges parallel to $0y$. Each element is characterized by an elastic constant g. The elasticity equations given in detail in Ref. [10] determine the strain and stress on each element of the network and are solved using a gradient conjugate method with error criterion 10^{-20}. As the applied deformation increases, a rupture occurs in an element i when its stress σ_i reaches a critical value σ_c. The novel rule that we add to describe earthquakelike events is to associate to each rupture an irreversible incremental deformation $w_s = \beta w_e$ in the broken plaquette, where $w_e = \sigma_c/g$ is the elastic deformation of the plaquette just prior to the rupture and $0 \leq \beta \leq 2$ is a parameter of the model. This irreversible deformation represents the slip associated with an earthquake. Imposing the slip w_s corresponds to adding a permanent force dipole of magnitude $f = g w_s$ which opposes the stress. As a consequence, the elastic stress in the element is instantaneously relaxed to a value equal to $\sigma_c(1-\beta/2)$ in an infinite system, and close to this value up to finite size corrections in a finite system. The stress distribution throughout the lattice is then adjusted instantaneously after each rupture according to the equations of equilibrium elasticity, and at the positions of increased stress, further rupture can occur leading to a chain reaction, a model earthquake. In the present "dislocation" model, we do not describe the details of the dynamical process of rupture: This corresponds to treating the velocity of sound as infinitely large, or better, to considering time scales larger than the few seconds to minutes that an earthquake lasts, such that the stress has had time to equilibrate everywhere.

After rupture, the element which has broken suffers no change in its material properties and it can support stress again in the future. This is the key difference with previous models [9,12] which assigned a new random stress threshold after each rupture event ("annealed" disorder). The physics underlying our assumption is that the slip associated with an individual earthquake is too small (a few meters for a fault of a few hundred kilometers) to induce a significant change of the mechanical properties of the gouge and barriers which control the stick-slip behavior of the element. Finally, the stress thresholds σ_c for each element are drawn once for all from a probability distribution $P_\sigma(\sigma)$ chosen uniform in the interval $[1-\Delta\sigma/2, 1+\Delta\sigma/2]$ with the value of $\Delta\sigma$ between 0.1 and 1.99 in the simulations that have been carried out. To summarize, our *deterministic* model belongs to the class of "sandpile" models [13] for self-organized criticality, characterized by slow driving and threshold dynamics, with, however, two additional ingredients, namely,

0031-9007/93/71(21)/3604(4)$06.00

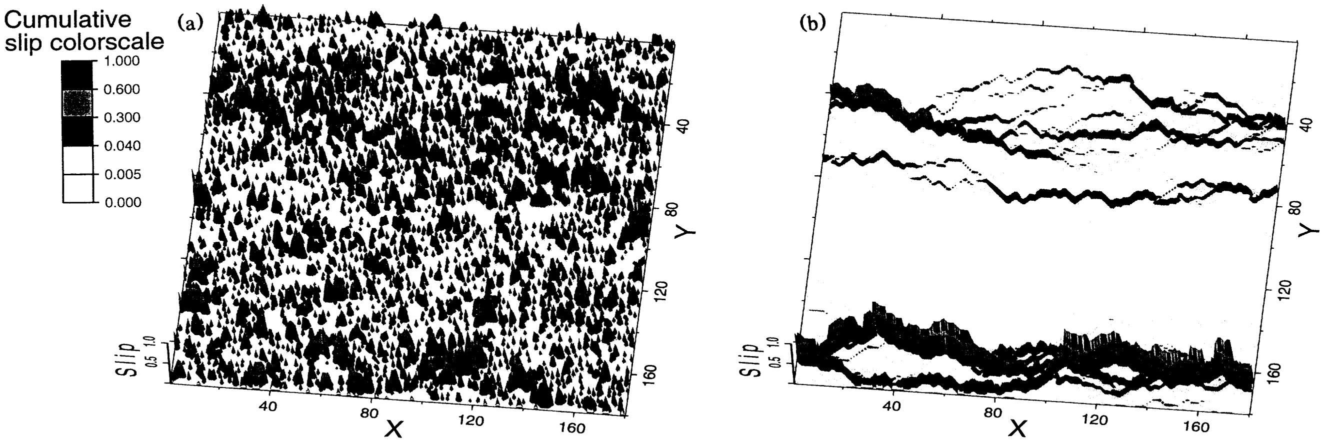

FIG. 1. Evolution of the cumulative earthquake slip, represented along the vertical axis in the white to black color code shown above the picture, at two different times: (a) early time and (b) long time, in a system of size $L=90$ by $L=90$, where $\Delta\sigma=1.9$ and $\beta=0.1$.

quenched disorder and long-range elastic forces.

At time $t=0$, the constant velocity boundary condition is switched on to some small value $V=10^{-3}$. Figure 1 shows the evolution of rupture at a short time [Fig. 1(a)] and a long time [Fig. 1(b)] in a system of size $L=90$ by $L=90$. At short times, a diffuse damage is observed where rupture reveals the weakest elements, distributed within the system in an uncorrelated way. As the deformation increases, clusters of elements which have ruptured begin to appear, grow, and coalesce. Elements on which the rupture activity is recurrent are found to organize in 1D lines, i.e., model faults, while the rupture activity progressively disappears in the other elements. Contrary to a common belief that localization appears either on preexisting weak structures and/or as a result of the change (i.e., weakening) of mechanical properties of the ruptured elements which tends to favor additional rupture, the localization observed in our model appears as a result of a slowly convergent dynamical optimization process, through which the system tends to organize in a state of marginal stability reminiscent of self-organized criticality in sandpile models [2,13].

The concept that faults are optimal structures is demonstrated by comparing Fig. 1(b) with Fig. 2 which shows the set of minimal directed paths in the same disorder landscape. More precisely, consider the 2D lattice where each bond is assigned a random weight, here the chosen stress threshold σ_c for each bond drawn once for all from the probability distribution $P_\sigma(\sigma)$. To each oriented path $P\{z(x)\}$ which cuts the lattice into two pieces, we can associate an "energy" $e(P)$ as the sum of the random weight of the bonds which constitute this path P. The minimum interface problem consists in finding the path P^* which possesses the smallest "energy" over all possible paths. The same problem has been investigated in another context as a limiting case, namely, in the statistical physics of a polymer interacting with a random mediim [14] in the limit $T \rightarrow 0$. This problem has been extensively studied as a baby model of the more general problem of the physics of complex disordered systems.

The set of optimal directed paths presented in Fig. 2 is obtained using a transfer-operator approach [15], modified to impose in addition that the path be periodic in accordance with the chosen periodic conditions along the vertical boundaries of our model. It relies on the chain property

$$e(x_1,z_1;x_2,z_2)=\min_{z'}[e(x_1,z_1;x',z')+e(x',z';x_2,z_2)]\,. \tag{1}$$

Figure 2 thus represents the 90 periodic optimal paths in a system of size $L=90$ by $L=90$, starting from $(x=1,z)$ and ending at $(x=L,z)$ for $z=1$ to 90. The path num-

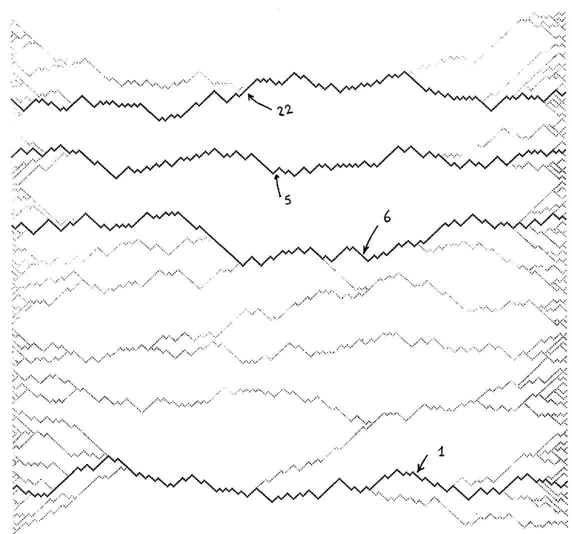

FIG. 2. Set of minimal directed paths in the same disorder "landscape" as for Fig. 1.

bered "1" in black is the one which has the smallest "energy" among all other paths. A striking first observation is the one to one correspondence between the most active fault seen in Fig. 1(b) and the best optimal path "1" drawn in Fig. 2, as can be seen by superposing the two figures. We have observed that this correspondence holds true for all realizations that have been explored as long as the degree β of stress release is smaller than the strength of disorder $\Delta\sigma$. For larger β, fault structures may be more complicated than a single path. We also note that the most active secondary faults found for larger values of β (see below) are coincident in part or as a whole with secondary optimal paths shown in Fig. 2.

In order to rationalize this remarkable correspondence, consider the limit of relatively large disorder $\Delta\sigma$ and small degree β of stress release. Consider an element which ends up belonging to an active fault. When the tectonic velocity is switched on at $t=0$, its stress begins to increase steadily until it reaches its threshold. Afterwards, being continuously driven to its stress threshold of instability, it will undergo oscillations of relaxation of small stress amplitude $\beta\sigma_c$. In the limit of small β, the stress-strain characteristic of the element approaches a horizontal line as $\beta \rightarrow 0$. The element behavior is thus close to being perfectly elastic plastic. This reasoning allows us to map the determination of the fault geometry in the limit $\beta \rightarrow 0$ to that of the set of connected elements just reaching their plastic thresholds, corresponding to the global network elastic-plastic yield point. When such a set appears in the network, the stress cannot increase further by definition. This maximum stress must be equal to the sum of the threshold values of each bond along the path. The path which first reaches the plastic regime for all bonds along its length is the one which minimizes the sum of stress thresholds along it [16] Q.E.D. It is important to underline that fault localization is deeply related to the existence of two fundamental features of the model, namely, long-range elastic forces and quenched disorder. In particular, the long-range elastic forces are responsible for screening by active faults which thus provide a positive feedback on the faults themselves.

Let us summarize briefly the different regimes found in various systems, with different sizes from 4×4 up to 90×90, with different parameters $0 \leq \beta \leq 2$ and $0.01 \leq \Delta\sigma \leq 1.9$. A systematic exploration shows that as long as $\beta < \Delta\sigma$ (the genuine geophysical situation), the deformation and rupture events are localized on optimal paths, possibly competing at long time scales. For $\beta < \Delta\sigma/10$ typically, the localization is extremely strong and the optimal path or fault dominates and takes up all the deformation. For larger values of β but still smaller than $\Delta\sigma$, we observe a localization of the deformation on a few optimal paths which compete in time, the fraction of slip occurring of one fault being comparable to that occurring on the competing fault. These results are, however, strongly dependent on the specific disorder configuration and large fluctuations from sample to sample are observed, which are typical of the hierarchical structure of optimal paths in random media, as seen, for instance, in Fig. 2. For $\beta > \Delta\sigma$, we observe another regime where the rupture events and the deformation become delocalized over wide set of bonds.

Another clear feature coming out of the simulations is the fact that the parameter β is similar to a temperature, in the sense that the larger β is the larger the fluctuations of the various variables of the problems, such as the elastic stress and strain fields. A precise quantification of these fluctuations is provided by the total elastic energy stored in the whole system. As a function of time, it exhibits small fluctuations for small β going to zero as $\beta \rightarrow 0$ and larger and larger fluctuations as β increases. This is compatible with the idea that β controls the degree of chaoticity of the model (the Lyapunov exponent increases with β) and can thus be viewed as a kind of effective temperature. The transition to a delocalized regime for $\beta > \Delta\sigma$ is also another good indication of this idea. For $\beta < \Delta\sigma$ but not small, localization occurs not on a single fault but on an ensemble of competing paths, which are in general separated by distances of the order of the system size. This can already be seen in Fig. 1(b): In this system realization, in addition to the well-defined fault at the bottom, a more complex fault structure has formed at the top. One fault system is typically active for very long periods of time (much larger than the longest time scale $\sim V^{-1}$ introduced by the tectonic velocity V) until the locus of ruptures spontaneously switches to a different fault(s) and the previously active fault may become completely silent for a long time. In some cases, the switch to another structure is brief. This feature of alternate fault activity over long periods of time has been described in several geological contexts and its origin is still a mystery. Here, these observations find a natural explanation within the analogy developed above with random directed polymers and viewing β as an effective temperature. Qualitatively, when several faults have almost the same "energy" and are thus almost equally optimal, we can understand qualitatively the competition between them as resulting from a slow exploration of these "energy" minima in the presence of a nonzero "temperature" β. Here, we dwell on the analogy with the random director polymer problem and note that the underlying chaotic "earthquake" dynamics [17] is similar to the thermal activation of the motion of a polymer due to the coupling to a thermal bath at a nonzero temperature T. If $T=0$, we recover the unique optimal path configuration. If $T > 0$, the polymer explores slowly a number of other configurations with a probability governed by the Boltzmann factor $e^{-e/k_B T}$. The long time scale of the switch of activity between distinct fault systems reflects the hierarchical [14] or ultrametric [18] structure of the "energy" landscape of the set of paths.

The present plate tectonic model provides a physical mechanism to explain the spontaneous formation of self-affine faults. It can be shown exactly [19], using a mapping onto the randomly stirred hydrodynamic Burger's equation, that random directed polymers are self-affine with a roughness exponent $\zeta = \frac{2}{3}$; i.e., the average width h of the transverse fluctuations of an optimal path of horizontal length L scales as $h \sim L^{\zeta}$. We have checked that the dynamically selected fault in the limit of small β is indeed self-affine with the exponent $\frac{2}{3}$ in two ways: (i) using the one to one correspondence between each bond of the optimal path and each corresponding bond in the dynamically selected fault and (ii) calculating directly the rms amplitude h of the transverse wandering of a fault as a function of its length L. This result can explain the formation of relatively well-defined faults which tend to grow and organize, not as straight objects, but more often as self-affine structures composed of many strands of varying lengths, leading to the geological concepts of fault segments and barriers. Furthermore, when the stress release parameter β is larger, faults come in groups and form a mulifractal structure, the geometry being the set of elements persistently breaking, the measure being the cumulative slip on each element. A thorough study of the multiscaling properties of these structures will be reported elsewhere but we note here that the complex fault structures which are dynamically selected bear resemblance to fractal fault patterns observed in nature [6,20] and in analog laboratory experiments [21,22].

We now turn to a brief description of the short-time dynamics on these fault structures. The model earthquakes are separated by wildy varying periods of time when few or no ruptures occur. We measure the elastic energy stored in the system just before and after an "earthquake," and assign the difference as being the energy release induced by the earthquake. These energy releases are found to follow a power-law distribution similar to the Gutenberg-Richter law over more than two decades, where the number $N(E)$ of earthquakes of energy E scales as

$$N(E) \sim E^{-(1+B)} \text{ with } B \approx 0.31 \pm 0.04 . \qquad (2)$$

We find that the exponent B is not sensitive to the value of the disorder parameter $\Delta\sigma$ and to the value of the degree β of stress release. A similar value $B \approx 0.3$ has been found in two different models, one [9] with "annealed" noise instead of quenched disorder and the other [12] using a tensorial elasticity with "annealed" noise. This suggests the existence of a kind of universality such that the critical exponent B seems insensitive to the nature of the disorder ("quenched" or "annealed") and to the scalar or tensorial nature of the field.

In summary, our result suggests the novel concept that individual faults are optimal interface structures, which entails their self-affine scaling and the multfractal structure of fault networks [3,4,20,21]. Finally, we note that the present model can also be used to describe the slow deformation and organization of slips stemming from microplasticity in polycrystals.

Laboratoire de Physique de la Matière Condensée is CNRS URA 190.

[1] G. C. P. King, R. S. Stein, and J. B. Rundle, J. Geophys. Res. **93**, 13307 (1988).
[2] A. Sornette and D. Sornette, Europhys. Lett. **9**, 197–202 (1989).
[3] C. Scholz, *The Mechanics of Earthquakes and Faulting* (Cambridge Univ. Press, Cambridge, 1990).
[4] D. Sornette, in *Spontaneous Formation of Space-Time Structures and Criticality*, edited by T. Riste and D. Sherringon, NATO ASI (Kluwer Academic, Norwell, MA, 1991), pp. 57–106.
[5] D. Sornette and J. Virieux, Nature (London) **357**, 401–403 (1992).
[6] D. T. Turcotte, in *Fractals in Geophysics*, edited by C. H. Scholz and B. B. Mandelbrot (Birkhäuser, Cambridge, 1989), pp. 171–196.
[7] J. M. Carlson and J. S. Langer, Phys. Rev. A **40**, 6470–6484 (1989).
[8] A. Crisanti, M. H. Jensen, A. Vulpiani, and G. Paladin, Phys. Rev. A **46**, R7363 (1992).
[9] K. Chen, P. Bak, and S. P. Obukhov, Phys. Rev. A **43**, 625–630 (1991).
[10] D. Sornette, C. Vanneste, and L. Knopoff, Phys. Rev. A **45**, 8351–8357 (1992).
[11] P. Cowie, C. Vanneste, and D. Sornette, J. Geophys. Res. (to be published).
[12] H-J. Xu, B. Bergersen, and K. Chen, J. Phys. A **25**, L1251 (1992).
[13] P. Bak, C. Tang, and K. Wiesenfeld, Phys. Rev. A **38**, 364 (1988).
[14] M. Kardar and Y.-C. Zhang, Phys. Rev. Lett. **58**, 2087 (1987).
[15] B. Derrida and J. Vannimenus, Phys. Rev. B **27**, 4401 (1983).
[16] S. Roux and A. Hansen, J. Phys. II (France) **2**, 1007–1021 (1992).
[17] To test the chaotic nature of the model, it is not possible to use the standard method involving the linearized dynamics for the computation of the Lyapunov exponents, since we cannot write the time evolution in terms of an explicit map. However, one can follow the divergence of nearby trajectories, and thus determine the maximum Lyapunov exponent. We have followed the procedure proposed in Ref. [8] for a cellular automation model of earthquakes. For a very large range of disorder $\Delta\sigma$ and stress release β parameters, the maximum Lyapunov exponent is found positive, indicating that deterministic chaos is a generic feature of the model.
[18] M. Mézard, G. Parisi, and M. A. Virasoro, *Spin Glass Theory and Beyond* (World Scientific, Singapore, 1987).
[19] D. A. Huse, C. L. Henley, and D. S. Fisher, Phys. Rev. Lett. **55**, 2924 (1985).
[20] C. H. Scholz and B. B. Mandelbrot, in *Fractals in Geophysics* (Ref. [6]).
[21] P. Davy, A. Sornette, and D. Sornette, Nature (London) **348**, 56 (1990).
[22] A. Sornette, P. Davy, and D. Sornette, Phys. Rev. Lett. **65**, 2266 (1990).

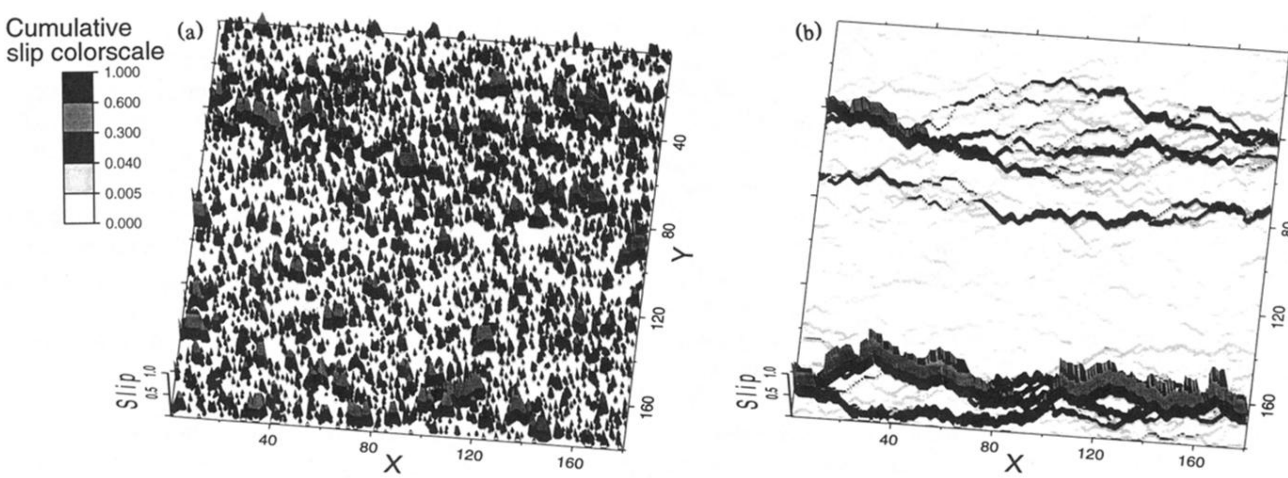

FIG. 1. Evolution of the cumulative earthquake slip, represented along the vertical axis in the white to black color code shown above the picture, at two different times: (a) early time and (b) long time, in a system of size $L=90$ by $L=90$, where $\Delta\sigma=1.9$ and $\beta=0.1$.